

**MATHEMATICAL MODELLING OF  
UNSTEADY NANOFLUID FLOW FOR HEAT,  
MASS AND MICROORGANISM TRANSFERS  
WITH MAGNETIC AND SLIP EFFECTS**

**NUR AMALINA BINTI ABDUL LATIFF**

**UNIVERSITI SAINS MALAYSIA**

**2018**

**MATHEMATICAL MODELLING OF  
UNSTEADY NANOFLUID FLOW FOR HEAT,  
MASS AND MICROORGANISM TRANSFERS  
WITH MAGNETIC AND SLIP EFFECTS**

by

**NUR AMALINA BINTI ABDUL LATIFF**

**Thesis submitted in fulfilment of the requirements  
for the degree of  
Doctor of Philosophy**

**August 2018**

## ACKNOWLEDGEMENT

*Bismillahirrahmanirrahim...*

All praise is due to Allah, the Lord of the world. Thanks to Allah for His love, care, and blessing in helping me to successfully complete this PhD thesis. To those who have accompanied, supported, and helped me to get through all the challenges during these few years, I would like to acknowledge their contributions.

To my supervisor, Professor Dr. Ahmad Izani Bin Md. Ismail, I would like to express my gratitude to his knowledge sharing, advice, and encouragement throughout the completion of this thesis. Thank you for always keeping an eye on my progress and always be there whenever needed. To my field-supervisor, Professor Dr. Md. Jashim Uddin, I appreciate his expert advice on modelling. Without the guidance from both of them, this PhD project would not be possible.

I would like to thank MyBrain15 (MyPhD) under the Ministry of Higher Education (MOHE) in providing the financial means for me to pursue this study. Furthermore, I would like to thank Universiti Sains Malaysia for providing the special provision RU funds (1001/PMATHS/8011013) for this project.

My deepest and eternal gratitude goes to my family, who provide all the love, encouragement, and prayers. To my fellow friends, they have my deep sense of gratitude for staying by my side even at my lowest point in life. Thanks to all of you who teach me all the good things that really matter in life. I don't think I could complete this thesis without their constant moral support. Thanks all!

## TABLE OF CONTENTS

Acknowledgement	ii
Table of Contents	iii
List of Tables	vii
List of Figures	ix
List of Symbols	xiv
Abstrak	xix
Abstract	xxi
<b>CHAPTER 1 - INTRODUCTION</b>	<b>1</b>
1.1 Research Background	1
1.1.1 Newtonian and Non-Newtonian Fluids	2
1.1.2 Nanoparticle and Microorganism	3
1.1.3 Magnetohydrodynamics	4
1.1.4 Unsteady Viscous Flow	5
1.1.5 Heat, Nanoparticle Mass, and Microorganism Transfers	6
1.1.6 Boundary Layer Theory	8
1.1.7 Dimensionless Number	10
1.1.8 Slip Boundary Conditions	14
1.1.9 Stefan Blowing Boundary Condition	15
1.2 Problem Statement	16
1.3 Research Objectives and Scope	17
1.4 Research Methodology	19
1.5 Significance of Study	21
1.6 Outline of Thesis	22

<b>CHAPTER 2 - LITERATURE REVIEW</b>	<b>25</b>
2.1 Introduction	25
2.2 Flow over Rotating Disk	25
2.3 Squeezing Flow between Two Parallel Disks	30
2.4 Flow over a Vertical Rotating Cone	33
2.5 Micropolar Flow over Stretching/Shrinking Sheet	36
2.6 The Effects of Stefan Blowing over Viscous Fluid	41
<b>CHAPTER 3 - GOVERNING EQUATIONS AND NUMERICAL METHOD</b>	<b>45</b>
3.1 Introduction	45
3.2 Governing Equations in Vector Form	45
3.3 Magnetic Field	47
3.4 Boussinesq Approximation	48
3.5 Unsteady MHD Nanofluid Flow over a Rotating Disk	50
3.6 Unsteady MHD Squeezing Nanofluid Flow between Two Parallel Disks	55
3.7 Unsteady MHD Nanofluid Flow over Rotating Cone	56
3.8 Unsteady MHD Mixed Convection Micropolar Nanofluid Flow over Vertical Stretching/Shrinking Sheet	57
3.9 Numerical Solution ( <i>dsolve</i> function)	68
3.9.1 Finite Difference Method	69
3.9.2 Richardson Extrapolation	71
3.9.3 Finite Difference Solution Procedure	73
<b>CHAPTER 4 - THE FORCED CONVECTIVE NANOFLUID FLOW WITH MICROORGANISM OVER A STRETCHABLE/SHRINKABLE ROTATING DISK</b>	<b>75</b>
4.1 Introduction	75

4.2	Problem Formulation	76
4.3	Similarity Transformations	78
4.4	Physical Quantities	80
4.5	Method of Solution	81
4.6	Comparison with Previous Literature	82
4.7	Results and Discussion	83
4.8	Conclusions	98
 <b>CHAPTER 5 - THE FORCED CONVECTION OF SQUEEZING NANOFLUID FLOW WITH MICROORGANISM BETWEEN TWO PARALLEL DISKS</b>		 <b>100</b>
5.1	Introduction	100
5.2	Problem Formulation	100
5.3	Similarity Transformations	103
5.4	Physical Quantities	105
5.5	Method of Solution	106
5.6	Comparison with Previous Literature	106
5.7	Results And Discussion	107
5.8	Conclusions	119
 <b>CHAPTER 6 - MIXED CONVECTION NANOFLUID FLOW WITH MICROORGANISM PAST A VERTICAL ROTATING CONE</b>		 <b>121</b>
6.1	Introduction	121
6.2	Problem Formulation	122
6.3	Similarity Transformations	124
6.4	Physical Quantities	126
6.5	Method of Solution	127
6.6	Comparison with Previous Literature	128

6.7	Results and Discussions	129
6.8	Conclusions	143
<b>CHAPTER 7 - MIXED CONVECTION MICROPOLAR NANOFLUID FLOW WITH MICROORGANISM OVER A VERTICAL STRETCHING OR SHRINKING SHEET</b>		<b>144</b>
7.1	Introduction	144
7.2	Problem Formulation	145
7.3	Similarity Transformations	147
7.4	Physical Quantities	150
7.5	Method of Solution	151
7.6	Comparison with Previous Literature	151
7.7	Results and Discussion	152
7.8	Conclusions	162
<b>CHAPTER 8 - CONCLUSIONS</b>		<b>163</b>
8.1	Summary of Research	163
8.2	Suggestion for Future Research	167
<b>REFERENCES</b>		<b>169</b>
<b>APPENDICES</b>		
<b>LIST OF PUBLICATIONS</b>		

## LIST OF TABLES

		Page
Table 4.1	The calculated values of $f''(0)$ and $g'(0)$ from the present model in the absence of energy, concentration, and microorganism equations	83
Table 4.2	Variations of $-f''(0)$ , $-g'(0)$ , $-\theta'(0)$ , $-\phi'(0)$ and $-\chi'(0)$ with $M$ and $S$ for different cases of $\lambda = -0.1, fw = -1$ , $\lambda = -0.1, fw = 1$ , $\lambda = 0.1, fw = -1$ , and $\lambda = 0.1, fw = 1$	95
Table 4.3	Variations of $-\theta'(0)$ , $-\phi'(0)$ and $-\chi'(0)$ with $\delta_u$ for different cases of $\lambda = -0.1, fw = -1$ , $\lambda = -0.1, fw = 1$ , $\lambda = 0.1, fw = -1$ , and $\lambda = 0.1, fw = 1$	96
Table 5.1	The comparison values of local skin friction of the present model with the previous literature for different values of $\lambda$ , $S$ , and $M$	107
Table 5.2	Variations of $-f''(1)$ , $-\theta'(1)$ , $-\phi'(1)$ and $-\chi'(1)$ with $\delta_u$ and $M$ for different cases of $S = -1, fw = -1$ ; $S = -1, fw = 1$ ; $S = 1, fw = -1$ and $S = 1, fw = 1$	116
Table 5.3	Variations of $-f''(1)$ , $-\phi'(1)$ and $-\chi'(1)$ with $\delta_T$ for different cases of $S = -1, fw = -1$ ; $S = -1, fw = 1$ ; $S = 1, fw = -1$ and $S = 1, fw = 1$	117
Table 6.1	Comparison of the skin friction in the $x$ -, $y$ - direction and local Nusselt number when varying of $Pr$ and $fw$	128
Table 6.2	Variations of $-g'(0)$ , $-\theta'(0)$ , $-\phi'(0)$ and $-\chi'(0)$ with $\delta_u$ for different cases of $\xi = 0.1, fw = -1$ , $\xi = 0.1, fw = 1$ , $\xi = 1, fw = -1$ and $\xi = 1, fw = 1$	135
Table 6.3	Variations of $-g'(0)$ , $-\theta'(0)$ , $-\phi'(0)$ and $-\chi'(0)$ with $Nr$ for different cases of $\xi = 0.1, fw = -1$ , $\xi = 0.1, fw = 1$ , $\xi = 1, fw = -1$ and $\xi = 1, fw = 1$	137
Table 6.4	Variations of $-g'(0)$ , $-\theta'(0)$ , $-\phi'(0)$ and $-\chi'(0)$ with $M$ for different cases of $\xi = 0.1, fw = -1$ , $\xi = 0.1, fw = 1$ , $\xi = 1, fw = -1$ and $\xi = 1, fw = 1$	138
Table 6.5	Variations of $-f''(0)$ , $-g'(0)$ , $-\phi'(0)$ and $-\chi'(0)$ with $\delta_T$ for different cases of $\xi = 0.1, fw = -1$ , $\xi = 0.1, fw = 1$ , $\xi = 1, fw = -1$ and $\xi = 1, fw = 1$	140



Table 6.6	Variations of $-f''(0)$ , $-g'(0)$ , $-\theta'(0)$ and $-\chi'(0)$ with $\delta_c$ for different cases of $\xi = 0.1, fw = -1$ , $\xi = 0.1, fw = 1$ , $\xi = 1, fw = -1$ and $\xi = 1, fw = 1$	141
Table 6.7	Variations of $-f''(0)$ , $-g'(0)$ , $-\theta'(0)$ and $-\phi'(0)$ with $\delta_n$ for different cases of $\xi = 0.1, fw = -1$ , $\xi = 0.1, fw = 1$ , $\xi = 1, fw = -1$ and $\xi = 1, fw = 1$	142
Table 7.1	Comparison values of local Nusselt number $-\theta'(0)$ in the absence of microorganism equation, velocity and thermal slip boundary when $\Delta_m = 0.1$ , $\lambda_0 = 1$ and $B = 0.1$	152
Table 7.2	Values of $h'(0)$ , $-\theta'(0)$ , $-\phi'(0)$ and $-\chi'(0)$ with $\delta_u$ for different cases of $\lambda = -0.1, fw = -0.1$ , $\lambda = -0.1, fw = -0.1$ , $\lambda = -0.1, fw = 0.1$ and $\lambda = 0.1, fw = -0.1$	159

## LIST OF FIGURES

		Page
Figure 1.1	The components of micromotor in a microfluidic system	2
Figure 1.2	Nanoparticle in the base fluid (Bucak, 2011)	4
Figure 1.3	Bioconvection process (Khan and Makinde, 2014)	7
Figure 1.4	Boundary layer profile (Groh, 2012)	9
Figure 1.5	The difference between no-slip velocity and slip velocity boundary layers (Maynes and Crockett, 2014)	14
Figure 1.6	The difference between no-slip (temperature, nanoparticle mass and microorganism) and slip (temperature, nanoparticle mass and microorganism) boundary layers (Maynes and Crockett, 2014)	15
Figure 1.7	Research framework	20
Figure 4.1	Physical model of rotating disk	76
Figure 4.2	Radial velocity profiles for various values of $M$ and $S$ for $\lambda = -0.1, f_w = -1$ case	85
Figure 4.3	Radial velocity profiles for various values of $M$ and $S$ for $\lambda = -0.1, f_w = 1$ case	85
Figure 4.4	Radial velocity profiles for various values of $M$ and $S$ for $\lambda = 0.1, f_w = -1$ case	86
Figure 4.5	Radial velocity profiles for various values of $M$ and $S$ for $\lambda = 0.1, f_w = 1$ case	86
Figure 4.6	Radial velocity profiles for various values of $\delta_u$ and different cases of $\lambda = -0.1, f_w = -1$ , $\lambda = -0.1, f_w = 1$ , $\lambda = 0.1, f_w = -1$ , and $\lambda = 0.1, f_w = 1$	87
Figure 4.7	Circumferential velocity profiles for various values of $\delta_u$ and different cases of $\lambda = -0.1, f_w = -1$ , $\lambda = -0.1, f_w = 1$ , $\lambda = 0.1, f_w = -1$ , and $\lambda = 0.1, f_w = 1$	88
Figure 4.8	Temperature profile for various values of $\delta_T$ and different cases of $\lambda = -0.1, f_w = -1$ , $\lambda = -0.1, f_w = 1$ , $\lambda = 0.1, f_w = -1$ , and $\lambda = 0.1, f_w = 1$	89

Figure 4.9	Nanoparticle mass profiles for various values of $\delta_C$ and different cases of $\lambda = -0.1, f_w = -1$ , $\lambda = -0.1, f_w = 1$ , $\lambda = 0.1, f_w = -1$ , and $\lambda = 0.1, f_w = 1$	89
Figure 4.10	Microorganism profiles for various values of $\delta_n$ and different cases of $\lambda = -0.1, f_w = -1$ , $\lambda = -0.1, f_w = 1$ , $\lambda = 0.1, f_w = -1$ , and $\lambda = 0.1, f_w = 1$	91
Figure 4.11	Effect of microorganism profiles for various values of Pé and different cases of $\lambda = -0.1, f_w = -1$ , $\lambda = -0.1, f_w = 1$ , $\lambda = 0.1, f_w = -1$ , and $\lambda = 0.1, f_w = 1$	91
Figure 4.12	Variations of the radial skin friction with $S$ for different values of $M$ and different cases of $\lambda = -0.1, f_w = -1$ , $\lambda = -0.1, f_w = 1$ , $\lambda = 0.1, f_w = -1$ , and $\lambda = 0.1, f_w = 1$	92
Figure 4.13	Variations of the circumferential skin friction with $S$ for different values of $M$ and different cases of $\lambda = -0.1, f_w = -1$ , $\lambda = -0.1, f_w = 1$ , $\lambda = 0.1, f_w = -1$ , and $\lambda = 0.1, f_w = 1$	93
Figure 4.14	Variations of the radial skin friction with $\delta_u$ for different cases of $\lambda = -0.1, f_w = -1$ , $\lambda = -0.1, f_w = 1$ , $\lambda = 0.1, f_w = -1$ , and $\lambda = 0.1, f_w = 1$	94
Figure 4.15	Variations of the circumferential skin friction with $\delta_u$ for different cases of $\lambda = -0.1, f_w = -1$ , $\lambda = -0.1, f_w = 1$ , $\lambda = 0.1, f_w = -1$ , and $\lambda = 0.1, f_w = 1$	94
Figure 4.16	Variation of the Nusselt number with $\delta_T$ for different cases of $\lambda = -0.1, f_w = -1$ , $\lambda = -0.1, f_w = 1$ , $\lambda = 0.1, f_w = -1$ , and $\lambda = 0.1, f_w = 1$	97
Figure 4.17	Variation of the Sherwood number with $\delta_C$ for different cases of $\lambda = -0.1, f_w = -1$ , $\lambda = -0.1, f_w = 1$ , $\lambda = 0.1, f_w = -1$ , and $\lambda = 0.1, f_w = 1$	97
Figure 4.18	Variation of the microorganism number with $\delta_n$ for different cases of $\lambda = -0.1, f_w = -1$ , $\lambda = -0.1, f_w = 1$ , $\lambda = 0.1, f_w = -1$ , and $\lambda = 0.1, f_w = 1$	98
Figure 5.1	Physical model of fluid flow between two parallel disks (Hatami and Ganji, 2014)	101
Figure 5.2	Velocity profiles for various values of $\delta_u$ , $M$ and for $S = -1, f_w = -1$ case	109

Figure 5.3	Velocity profiles for various values of $\delta_u$ , $M$ and for $S = -1, fw = 1$ case	109
Figure 5.4	Velocity profiles for various values of $\delta_u$ , $M$ and for $S = 1, fw = -1$ case	110
Figure 5.5	Velocity profiles for various values of $\delta_u$ , $M$ and for $S = 1, fw = 1$ case	110
Figure 5.6	Temperature profiles for various values of $\delta_T$ and different cases of $S = -1, fw = -1$ ; $S = -1, fw = 1$ ; $S = 1, fw = -1$ and $S = 1, fw = 1$	111
Figure 5.7	Nanoparticle mass profiles for various values of $\delta_C$ and different cases of $S = -1, fw = -1$ ; $S = -1, fw = 1$ ; $S = 1, fw = -1$ and $S = 1, fw = 1$	112
Figure 5.8	Microorganism profiles for various values of $\delta_n$ and different cases of $S = -1, fw = -1$ ; $S = -1, fw = 1$ ; $S = 1, fw = -1$ and $S = 1, fw = 1$	114
Figure 5.9	Variation of the upper disk skin friction with $M$ for different values of $\delta_u$ and different cases of $S = 1, fw = -1$ ; $S = -1, fw = 1$ ; $S = 1, fw = -1$ and $S = 1, fw = 1$	115
Figure 5.10	Variation of the upper disk Nusselt number for different values of $\delta_T$ and different cases of $S = -1, fw = -1$ ; $S = -1, fw = 1$ ; $S = 1, fw = -1$ and $S = 1, fw = 1$	115
Figure 5.11	Variation of the upper disk Sherwood number for different values of $\delta_C$ and different cases of $S = -1, fw = -1$ ; $S = -1, fw = 1$ ; $S = 1, fw = -1$ and $S = 1, fw = 1$	118
Figure 5.12	Variation of the upper disk microorganism number for different values of $\delta_n$ and different cases of $S = -1, fw = -1$ ; $S = -1, fw = 1$ ; $S = 1, fw = -1$ and $S = 1, fw = 1$	119
Figure 6.1	Physical model of the vertical rotating cone (Saleem and Nadeem, 2015)	122
Figure 6.2	Tangential velocity profiles for various values of $\delta_u$ and different cases of $\xi = 0.1, fw = -1$ , $\xi = 0.1, fw = 1$ , $\xi = 1, fw = -1$ and $\xi = 1, fw = 1$	130

Figure 6.3	Tangential velocity profiles for various values of $Nr$ and different cases of $\xi = 0.1, fw = -1$ , $\xi = 0.1, fw = 1$ , $\xi = 1, fw = -1$ and $\xi = 1, fw = 1$	131
Figure 6.4	Tangential velocity profiles for various values of $M$ and different cases of $\xi = 0.1, fw = -1$ , $\xi = 0.1, fw = 1$ , $\xi = 1, fw = -1$ and $\xi = 1, fw = 1$	131
Figure 6.5	Temperature profiles for various values of $\delta_T$ and different cases of $\xi = 0.1, fw = -1$ , $\xi = 0.1, fw = 1$ , $\xi = 1, fw = -1$ and $\xi = 1, fw = 1$	133
Figure 6.6	Nanoparticle mass profiles for various values of $\delta_C$ and different cases of $\xi = 0.1, fw = -1$ , $\xi = 0.1, fw = 1$ , $\xi = 1, fw = -1$ and $\xi = 1, fw = 1$	133
Figure 6.7	Microorganism profiles for various values of $\delta_n$ and different cases of $\xi = 0.1, fw = -1$ , $\xi = 0.1, fw = 1$ , $\xi = 1, fw = -1$ and $\xi = 1, fw = 1$	134
Figure 6.8	The primary (tangential) skin friction with $\delta_u$ and different cases of $\xi = 0.1, fw = -1$ , $\xi = 0.1, fw = 1$ , $\xi = 1, fw = -1$ and $\xi = 1, fw = 1$	135
Figure 6.9	The primary skin friction with $Nr$ and different cases of $\xi = 0.1, fw = -1$ , $\xi = 0.1, fw = 1$ , $\xi = 1, fw = -1$ and $\xi = 1, fw = 1$	137
Figure 6.10	Variation of the primary skin friction with $M$ and different cases of $\xi = 0.1, fw = -1$ , $\xi = 0.1, fw = 1$ , $\xi = 1, fw = -1$ and $\xi = 1, fw = 1$	138
Figure 6.11	Variation of the Nusselt number with $\delta_T$ and different cases of $\xi = 0.1, fw = -1$ , $\xi = 0.1, fw = 1$ , $\xi = 1, fw = -1$ and $\xi = 1, fw = 1$	140
Figure 6.12	Variation of the Sherwood number with $\delta_C$ and different cases of $\xi = 0.1, fw = -1$ , $\xi = 0.1, fw = 1$ , $\xi = 1, fw = -1$ and $\xi = 1, fw = 1$	141
Figure 6.13	Variation of the microorganism number with $\delta_n$ and different cases of $\xi = 0.1, fw = -1$ , $\xi = 0.1, fw = 1$ , $\xi = 1, fw = -1$ and $\xi = 1, fw = 1$	142
Figure 7.1	Physical model of stretching/shrinking sheet	145

Figure 7.2	Velocity profiles for various values of $\xi$ for different cases of $\lambda = -0.1, fw = -0.1$ , $\lambda = -0.1, fw = -0.1$ , $\lambda = -0.1, fw = 0.1$ and $\lambda = 0.1, fw = -0.1$	153
Figure 7.3	Velocity profiles for various values of $M$ for different cases of $\lambda = -0.1, fw = -0.1$ , $\lambda = -0.1, fw = -0.1$ , $\lambda = -0.1, fw = 0.1$ and $\lambda = 0.1, fw = -0.1$	155
Figure 7.4	Velocity profiles for various values of $\delta_u$ for different cases of $\lambda = -0.1, fw = -0.1$ , $\lambda = -0.1, fw = -0.1$ , $\lambda = -0.1, fw = 0.1$ and $\lambda = 0.1, fw = -0.1$	155
Figure 7.5	Microrotation profiles for various values of $\Delta_m$ for different cases of $\lambda = -0.1, fw = -0.1$ , $\lambda = -0.1, fw = -0.1$ , $\lambda = -0.1, fw = 0.1$ and $\lambda = 0.1, fw = -0.1$	156
Figure 7.6	Temperature profiles for various values of $\delta_T$ for different cases of $\lambda = -0.1, fw = -0.1$ , $\lambda = -0.1, fw = -0.1$ , $\lambda = -0.1, fw = 0.1$ and $\lambda = 0.1, fw = -0.1$	157
Figure 7.7	Concentration profiles for various values of $\delta_C$ for different cases of $\lambda = -0.1, fw = -0.1$ , $\lambda = -0.1, fw = -0.1$ , $\lambda = -0.1, fw = 0.1$ and $\lambda = 0.1, fw = -0.1$	157
Figure 7.8	Microorganism profiles for various values of $\delta_n$ for different cases of $\lambda = -0.1, fw = -0.1$ , $\lambda = -0.1, fw = -0.1$ , $\lambda = -0.1, fw = 0.1$ and $\lambda = 0.1, fw = -0.1$	158
Figure 7.9	Variation of the skin friction with $\delta_u$ for different cases of $\lambda = -0.1, fw = -0.1$ , $\lambda = -0.1, fw = -0.1$ , $\lambda = -0.1, fw = 0.1$ and $\lambda = 0.1, fw = -0.1$	160
Figure 7.10	Variation of the Nusselt number with $\delta_T$ and different cases of $\lambda = -0.1, fw = -0.1$ , $\lambda = -0.1, fw = -0.1$ , $\lambda = -0.1, fw = 0.1$ and $\lambda = 0.1, fw = -0.1$	160
Figure 7.11	Variation of the Sherwood number with $\delta_C$ for different cases of $\lambda = -0.1, fw = -0.1$ , $\lambda = -0.1, fw = -0.1$ , $\lambda = -0.1, fw = 0.1$ and $\lambda = 0.1, fw = -0.1$	161
Figure 7.12	Variation of the microorganism number with $\delta_n$ for different cases of $\lambda = -0.1, fw = -0.1$ , $\lambda = -0.1, fw = -0.1$ , $\lambda = -0.1, fw = 0.1$ and $\lambda = 0.1, fw = -0.1$	161

## LIST OF SYMBOLS

$a$	characteristic parameter ( $s^{-1}$ )
$\tilde{b}$	chemotaxis constant ( $m$ )
$B$	variable magnetic field strength ( <i>tesla</i> )
$B_0$	constant magnetic field strength ( <i>tesla</i> )
$C_{f\bar{r}}$	local skin friction coefficient (-)
$C$	nanoparticle mass (-)
$C_L$	lower disk nanoparticle mass (-)
$C_U$	upper disk nanoparticle mass (-)
$C_w$	wall nanoparticle mass (-)
$D_1$	local thermal slip parameter ( $m$ )
$D_B$	Brownian diffusion coefficient ( $m^2s^{-1}$ )
$D_T$	thermophoretic diffusion coefficient ( $m^2s^{-1}$ )
$D_n$	microorganism diffusion coefficient ( $m^2s^{-1}$ )
$E_1$	local nanoparticle mass slip parameter ( $m$ )
$f(\eta)$	dimensionless stream function (-)
$fw$	suction/injection velocity
$F_1$	local microorganism slip parameter ( $m$ )
$Gr$	Grashoff number (-)
$h(t)$	variable film thickness (-)

$j$	micro inertia density ( $m^2$ )
$k$	thermal conductivity of the fluid ( $Wm^{-1}K^{-1}$ )
$Le$	Lewis number (-)
$Lb$	bio-convection Lewis number (-)
$m_w$	surface mass flux
$M$	magnetic field parameter (-)
$n$	number of motile microorganism (-)
$n_m$	particle concentration difference (-)
$n_L$	number of motile microorganism at lower disk (-)
$n_U$	number of motile microorganism at upper disk (-)
$n_w$	wall motile microorganisms (-)
$N_1$	local $u$ -velocity slip factor ( $sm^{-1}$ )
$N_2$	local $v$ -velocity slip factor ( $sm^{-1}$ )
$Nb$	Brownian motion parameter (-)
$Nt$	thermophoresis parameter (-)
$Nu_{\bar{r}} / Nu_{\bar{x}}$	local Nusselt number (-)
$Pé$	bio-convection Péclet number (-)
$Pr$	Prandtl number (-)
$q_w$	surface heat flux ( $Wm^{-2}$ )
$q_n$	surface micro-organism flux (-)



$Q_{nr} / Q_{nx}$	local microorganism number (-)
$\bar{r}$	dimensional disk radial coordinate ( $m$ )
$Rb$	bioconvection Rayleigh number (-)
$Re_{\bar{r}} / Re_{\bar{x}}$	usual Reynolds number (-)
$S / s$	unsteadiness parameter (-)
$Sh_{\bar{r}} / Sh_{\bar{x}}$	local Sherwood number (-)
$\bar{t}$	dimensional time ( $s$ )
$T$	nanofluid temperature ( $K$ )
$T_L$	lower disk temperature ( $K$ )
$T_U$	upper disk temperature ( $K$ )
$T_w$	wall disk temperature ( $K$ )
$\bar{u}$	velocity component along the Cartesian coordinate $\bar{x}$ - axis ( $ms^{-1}$ )
$\bar{u}_{\bar{r}}$	velocity component along the cylindrical coordinate $\bar{r}$ - axis ( $ms^{-1}$ )
$\bar{u}_{\theta}$	velocity component along the cylindrical coordinate $\theta$ - axis ( $ms^{-1}$ )
$\bar{u}_{\bar{z}}$	velocity component along the cylindrical coordinate $\bar{z}$ - axis ( $ms^{-1}$ )
$\bar{v}$	velocity component along the Cartesian coordinate $\bar{y}$ - axis ( $ms^{-1}$ )
$\bar{w}$	velocity component along the Cartesian coordinate $\bar{z}$ - axis ( $ms^{-1}$ )
$W_c$	maximum cell swimming speed ( $ms^{-1}$ )
$\bar{z}$	dimensional coordinate along the plate ( $m$ )
$\Delta_m$	micropolar parameter

$\Omega$	angular velocity ( $ms^{-1}$ )
$\Omega_1$	rotational angular velocity about axis of cone ( $ms^{-1}$ )
$\Omega_2$	rotational velocity about point $O$ of cone ( $ms^{-1}$ )
$\alpha$	thermal conductivity ( $m^2s^{-1}$ )
$\alpha^*$	semi-vertical angle of the cone.
$\beta$	volumetric thermal expansion coefficient
$\beta_0$	characteristics length ( $m$ )
$\chi(\eta)$	dimensionless number of motile microorganism ( $-$ )
$\delta_c$	nanoparticle slip parameter ( $-$ )
$\delta_n$	microorganism slip parameter ( $-$ )
$\delta_T$	thermal slip parameter ( $-$ )
$\delta_u$	$u$ -velocity slip parameter ( $-$ )
$\delta_v$	$v$ -velocity slip parameter ( $-$ )
$\phi(\eta)$	dimensionless nanoparticle mass ( $-$ )
$\eta$	independent similarity variable ( $-$ )
$\kappa$	vortex viscosity coefficient ( $kg\ m^{-1}\ s^{-1}$ )
$\lambda$	stretching/shrinking parameter ( $-$ )
$\mu$	absolute viscosity of the fluid ( $kg\ m^{-1}\ s^{-1}$ )
$\nu$	kinematic viscosity ( $m^2s^{-1}$ )
$\theta(\eta)$	dimensionless temperature ( $-$ )

$\rho$	nanofluid density ( $kg\ m^{-3}$ )
$\sigma$	variable electric conductivity ( <i>siemens</i> $m^{-1}$ )
$\tau$	ratio of the effective heat capacity of the nanoparticle material to the fluid heat capacity ( $Nm^{-2}$ )
$\tau_{rz} / \tau_{xz}$	shear stress in $\bar{r}, \bar{z}$ -direction or $\bar{r}, \bar{x}$ -direction ( $Nm^{-2}$ )
$\xi$	mixed convection parameter (-)
$\psi$	stream function ( $m^2s^{-1}$ )
$( )'$	ordinary differentiation with respect to $\eta$ .

**PEMODELAN MATEMATIK BAGI ALIRAN NANOBENDALIR TAK  
MANTAP UNTUK PEMINDAHAN HABA, JISIM DAN  
MIKROORGANISMA DENGAN KESAN  
MAGNETIK DAN GELINCIRAN**

**ABSTRAK**

Kajian tentang masalah aliran dengan medan magnet, nanobendalir dan mikroorganisma adalah penting dan sering berfungsi dalam peranti mikrobendalir. Kelebihan peranti mikrobendalir adalah saiz kecil, kos rendah dan penggunaan tenaga rendah terutama untuk kajian biologi. Mikroorganisma dalam nanobendalir adalah penting untuk mencegah pengumpulan nanozarah, meningkatkan kestabilan nanobendalir, meningkatkan pencampuran dan dengan itu meningkatkan pemindahan jisim dalam peranti mikrobendalir. Tesis ini adalah kajian ke atas model matematik yang telah diubahsuai untuk mengkaji aliran lapisan sempadan untuk pemindahan haba, jisim nanozarah dan mikroorganisma dalam proses bio-kimia yang melibatkan peranti mikrobendalir. Masalah aliran nanobendalir spesifik ke atas pelbagai geometri seperti aliran ke atas cakera berputar yang boleh meregang dan mengecut, aliran di antara dua cakera selari, aliran melalui kon menegak berputar dan aliran nanobendalir mikrokutub ke atas lembaran yang boleh meregang dan mengecut telah diselidiki. Kesan magnetik, peniupan Stefan dan beberapa syarat sempadan gelincir (halaju gelincir, haba gelincir, jisim nanozarah gelincir dan mikroorganisma gelincir) dimasukkan ke dalam model. Kedua-dua nanobendalir yang Newtonan dan tak Newtonan (mikrokutub) telah diambil kira. Transformasi yang sesuai telah digunakan untuk mengubah persamaan pembezaan separa ke persamaan pembezaan biasa tak linear. Persamaan pembezaan biasa tak linear telah diselesaikan secara berangka

menggunakan kaedah beza sehingga ditambah dengan teknik ekstrapolasi Richardson dalam perisian Maple. Keputusan berangka yang diperoleh dalam kajian ini dibandingkan dengan kajian lepas dan keputusan perbandingan yang baik telah diperoleh. Kesan beberapa parameter kawalan pada halaju tanpa dimensi, suhu, jisim nanozarah, ketumpatan mikroorganisma serta kuantiti fizikal yang lain telah dikaji secara teliti melalui graf. Didapati kesan peniupan Stefan ke atas aliran bagi geometri lembaran mengecut dan cakera berputar mengecut telah menyediakan satu medium untuk meningkatkan geseran kulit manakala kesan penyedutan ke atas aliran bagi geometri lembaran meregang dan cakera berputar meregang dapat meningkatkan pemindahan haba, pemindahan jisim nanozarah dan pemindahan mikroorganisma. Bagi aliran antara dua cakera selari, pekali geseran kulit meningkat hasil apabila cakera atas bergerak ke arah bawah dengan kesan peniupan Stefan. Sementara itu, apabila cakera atas bergerak ke arah atas dengan kesan penyedutan, kadar pemindahan haba, kadar pemindahan jisim nanozarah dan kadar pemindahan mikroorganisma meningkat. Bagi aliran melewati kon berputar menegak, kesan peniupan Stefan meningkatkan pekali geseran kulit, kadar pemindahan haba, pemindahan jisim nanozarah dan pemindahan mikroorganisma apabila parameter konveksi bercampur meningkat. Masalah-masalah ini adalah relevan untuk meningkatkan prestasi peranti mikrobendalir yang bergantung kepada campuran air yang stabil daripada nanozarah magnetik dan mikroorganisma.

**MATHEMATICAL MODELLING OF UNSTEADY NANOFLUID FLOW  
FOR HEAT, MASS, AND MICROORGANISM TRANSFERS WITH  
MAGNETIC AND SLIP EFFECTS**

**ABSTRACT**

The study of flow problems related to the magnetic field, nanofluid, and microorganism are important especially in microfluidic devices. The advantages of microfluidic devices are its small size, low cost, and low consumption, especially for biological studies. The microorganisms in the nanofluid are essential to prevent nanoparticle agglomeration, to improve the stability of the nanofluids, to enhance mixing and hence enhance mass transfer in microfluidic devices. This thesis investigates the modified mathematical models to study the boundary layer flow for heat, nanoparticle mass, and microorganism transfers in the biochemical process involving microfluidic devices. Specific nanofluid flow problems under various geometries such as flow over stretchable/shrinkable rotating disk, flow between two parallel disks, flow over a vertical rotating cone, and micropolar nanofluid flow over a stretching/shrinking sheet were investigated. The effects of magnetic, Stefan blowing, and various slips (velocity slip, thermal slip, nanoparticle mass slip, and microorganism slip) were incorporated into the models. Both the Newtonian and non-Newtonian (micropolar) nanofluids have been taken into account. Appropriate transformations have been used to transform the partial differential equations into nonlinear ordinary differential equations. The differential equations have been solved numerically using the finite difference method coupled with the Richardson extrapolation technique in Maple software. The numerical results obtained in this study were compared with previous literature, and a good agreement

was found. The effect of controlling parameters on the dimensionless velocities, temperature, nanoparticle mass, the density of motile microorganisms, as well as other quantities of physical interest have been thoroughly examined via graphs. It was found that the effects of Stefan blowing on the flow over the shrinking sheet and shrinking rotating disk have been served as a medium to enhance the local skin friction, while the effects of suction on the same geometries elevate the heat, nanoparticle mass, and microorganism transfer. For the flow between two parallel disks, the skin friction coefficient increases as a result when the upper disk moves in the downward direction with blowing effect. Meanwhile, when the upper disk moves in the upward direction with suction effect, the rate of heat transfer, nanoparticle mass transfer, and microorganism transfer increase. For the flow over a vertical rotating cone, the effect of Stefan blowing enhances the skin friction coefficient, the rate of heat transfer, nanoparticle mass transfer, and microorganism transfer as the mixed convection parameter increases. These problems are relevant to improve the performance of the microfluidic device which is based on stable water suspensions of magnetic, nanoparticles, and microorganisms.

# CHAPTER 1

## INTRODUCTION

### 1.1 Research Background

Many studies have been conducted to explore the theory and basic physical principles in miniaturization and microfluidic applications. Microfluidics is the technology of driving and controlling fluids at the micrometer scale (Rusconi et al., 2014). The mixing process in the microfluidic device is vital to create Coriolis force and thus increases the contact surface between liquid molecules. This will enhance the effect of diffusion and advection. Due to this ability, micromixers can be applied for the purpose of fast heating and cooling reactions, such as handling hazardous substances and chemical reactions. The applications of microfluidic devices include in the production of colloidal systems or nanoparticles, production of the freeze-quenching process, the use in highly exothermal reactions, the synthesis of the biomolecule, the drug delivery systems, and the diagnostic testing (Teh et al., 2008).

Al-Halhouli et al. (2014) studied an application of micromotor system as a bioreactor for the cultivation of bacteria *S. cerevisiae*. It is one of the microfluidic applications involving magnetic field and microorganisms. Figure 1.1 shows a micromotor consists of a stator including double layer coils, and a rotor disk containing alternate permanent magnets for the cultivation of *S. cerevisiae*. From the extracted cultivation results, Al-Halhouli et al. (2014) suggested the use of the same concept for biotechnological applications like the cultivation of yeast cells. Furthermore, the results obtained had encouraged them to put further efforts towards the development



of electromagnetic based multifunction microfluidic platforms for lab-on-a-chip applications.

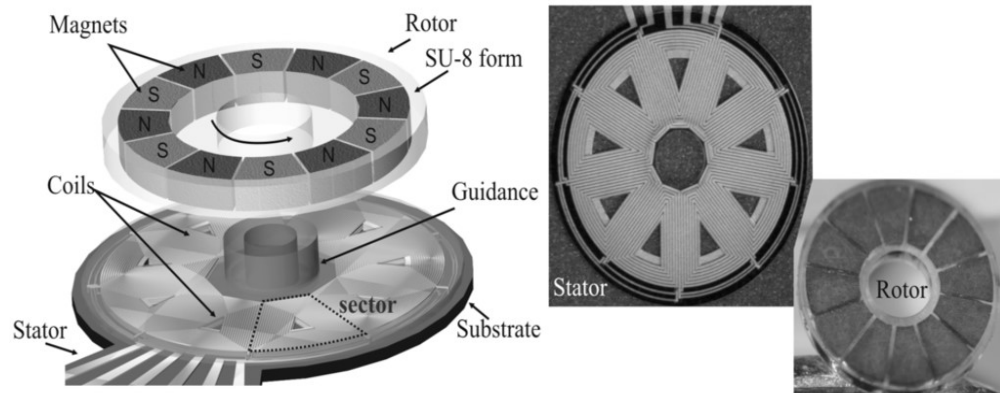


Figure 1.1 The components of micromotor in a microfluidic system (Al-Halhouli et al., 2014)

This thesis investigates the unsteady magnetohydrodynamic flow of a nanofluid containing nanoparticles and microorganisms over various geometries, including flow over the rotating stretchable/shrinkable disk, flow between two parallel disks, flow over the vertical rotating cone and stretching/shrinking sheet. The topics investigated are essential and have received much attention owing to potential applications in the design of microfluidic devices. The next subsection discusses specific basic concepts, principles, and phenomena involved with the background of this research.

### 1.1.1 Newtonian and Non-Newtonian Fluids

Al-Halhouli et al. (2014) pointed out that manipulating fluids at different viscosities for microfluidic systems in biomedical/biotechnological applications is a big challenge. Hence, this thesis considers both the Newtonian (water-based nanofluid) and non-Newtonian (micropolar nanofluid) fluid flow. Newton's law of

viscosity was introduced by Sir Isaac Newton stating that the shear stress is proportional to the shear rate. Fluids which obey this law are known as Newtonian fluids. Examples of Newtonian fluids include air and other gases, water, kerosene, gasoline, and other oil-based liquids. However, there are certain fluids such as polymeric suspensions, liquid crystal, and industrial colloids fluid, where the Newtonian fluid fails to describe the properties of these fluids. These types of fluid do not obey Newton's law whose flow curve (shear stress versus shear rate) is nonlinear and hence are called the non-Newtonian fluids. In most real cases, fluids including shampoo, ketchup, mud, paints, and cosmetic products have been widely used in many applications. These fluids are known as the micropolar fluids which are non-Newtonian fluids consisting of small body fluids and colloidal fluid elements (Rahman, 2009). These fluids cannot be easily represented or modelled as viscous fluids under Newton's law of motion or by the Navier-Stokes equations. Their special characters, such as small body fluids and colloidal fluid elements, need to be considered in understanding the motion of the fluid flow (Hussanan et al., 2017). Therefore, researchers realised that the studies of micropolar fluid flow are essential.

### **1.1.2 Nanoparticle and Microorganism**

Another modification that can be made to enhance the mixing process is by introducing nanoparticles and microorganisms into the microfluidic system. The term 'nanofluid' was first suggested by Choi and Eastman (1995) to describe pure fluids with suspended nanoparticles. He defined nanofluid as a fluid containing nanoscale-sized particles between 1 to 100 nm in the base fluids (water, oils, and ethylene glycol) (Rana and Bhargava, 2012) (Figure 1.2). Wang and Fan (2010) mentioned that manipulation of the structure and the distribution of nanoparticles can affect the

macroscopic properties of the nanofluid, such as its thermal conductivity. Nanoparticles are not self-propelled. Hence they just move due to such phenomena as Brownian motion and thermophoresis, carried by the flow of the base fluid.

Microorganisms in the nanofluid have the function to prevent nanoparticle agglomeration, to improve the stability of the nanofluids, and to enhance mixing and mass transfer (Uddin et al., 2016a; Khan and Makinde, 2014). Motile microorganisms can actively swim in the fluid in response to such stimuli as gravity, light, or chemical attraction. The combined benefits of nanoparticles and motile microorganisms in a suspension can be incorporated in microsystems.

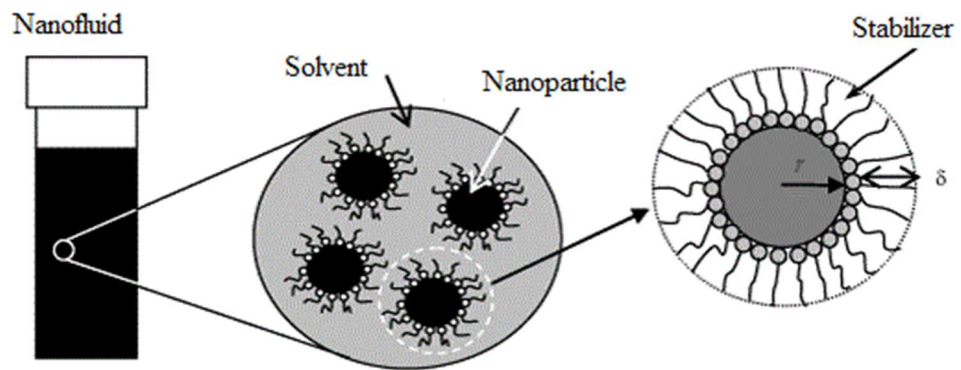


Figure 1.2 Nanoparticle in the base fluid (Bucak, 2011)

### 1.1.3 Magnetohydrodynamics

Magnetohydrodynamics (MHD) is a branch of physics that studies the dynamics of magnetic fields in electrically conducting fluids (Cristofolini, 2016). Lorentz force that considered to represent the effect of MHD in the mathematical models is consist of electric field and magnetic field. In this study, it is assumed that there is no polarised or applied voltage enforced on the fluid flow which imposes zero electric fields. The magnetic Reynolds number of the flow taken is small enough, allowing that only magnetic field could influence the Lorentz force. The magnetic

field effect plays an important role to enhance heat, nanoparticle mass, and microorganism transfer in microfluidic devices. According to Lin and Basuray (2011), the advantage of using external system with the magnetic field is the creation of Lorentz body forces to enhance the mixing. The mechanism involves a complex flow field induced by the magnetic field effect that can generate deformations and stretch the material interface between liquid molecules to enhance the mixing. Lu et al. (2001) used a rotating micromagnetic disk with an additional force driven by a commercial rotating magnet. Huh et al. (2008) has implemented a rotating micromagnetic disk driven by a rotating magnetic field. The detailed formulation of the magnetic field is explained in Section 3.3.

#### **1.1.4 Unsteady Viscous Flow**

Many researchers in the past have modelled a convective boundary layer flow by assuming a steady state. Having realised that, it is not possible to maintain a steady-state condition in the boundary layer fluid flow. Nowadays, many researchers have shown great interests to study the unsteady boundary layer flows. The steady state could not be maintained due to the impulsive change in the surface velocity or temperature (heat flux) involving the time-dependent variations (El-Aziz, 2013). There are other situations where unsteady situations need to be taken into account, such as self-induced motions of the body, fluctuations, and non-uniformities in the surrounding fluid. Furthermore, the unsteady analysis need to be considered when microorganism is introduced into a model, with the assumption that the concentration of microorganisms is high. This phenomenon is based on the observations from the experimental results which reported that an unsteady convection analysis is needed to

observe the collection of cloudy plumes microorganism as the concentration increased (Vadász, 2008).

### **1.1.5 Heat, Nanoparticle Mass, and Microorganism Transfers**

There are several types of convection which are free convection, forced convection, and mixed convection, to model heat, nanoparticle mass, and microorganism transfers. The natural (or free) convection deals with the flow induced by buoyancy forces, which arise from density differences caused by temperature, nanoparticle mass, and microorganism variations in the fluid. Forced convection occurs when the flow is created by external means, such as a fan, a pump, and other similar equipment. Mixed or combined convection occurred when the buoyancy forces exist as a result of the temperature, nanoparticle mass, and microorganism differences. Hence, this will induce the fluids to flow in free convection with a forced flow (Çengel and Cimbala, 2006). The effects of these buoyancy forces can be insignificant when the fluids considered are in a forced flow situation. However, in some cases, these buoyancy forces have a significant effect on heat, nanoparticle mass, and microorganism transfer rates in a flow (Shanmugapriya, 2008).

Heat transfer is the process of energy transfer between two bodies due to temperature and pressure differences. Heat is transferred from a higher temperature medium to a lower temperature medium. The thermal equilibrium is reached when all bodies involved, and the surroundings recorded the same temperature. The Second Law of Thermodynamics defines the concept of thermodynamic entropy to measure heat transfer. Mass transfer deals with the transport of material. Mass is transferred from high concentration region to low concentration region, the same mechanism as

heat transfer. The basic theory to explain the mass movement or flux is given by Fick's first law of diffusion. Fick's law states that the flux is proportional to the diffusivity and the negative gradient of concentration (Asano, 2007).

The behaviour of microorganisms can be observed using numerical and laboratory experimental results. Based on previous experimental results, it has been observed that one of the most remarkable behaviours of microorganisms is that they create bioconvection process (Clement et al., 1997; Shaw et al., 2014). Bioconvection is defined as the spontaneous pattern formation of motile microorganisms which are denser than water. The phenomena occurred due to motile microorganisms which swim and migrating upwards against gravity, and accumulating at the upper surface hence creating an unstable density stratification of the fluid. Rayleigh-Benard convection is the earliest and the most fundamental mechanism of bioconvection used to understand microorganisms transport. As the fluid layer is heated from below, microorganisms swim in an upward direction, and hence unstable density gradients occurred, and bioconvection process is observed (Figure 1.3).

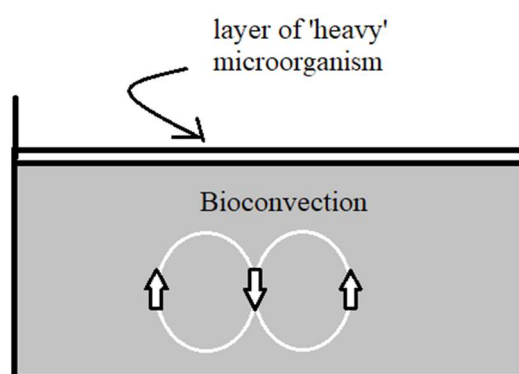


Figure 1.3 Bioconvection process (Khan and Makinde, 2014)

The ability of microorganism, which is self-propelling, plays a vital role in nature to transport diffusive substance such as salt and sugar. Microorganisms are classified according to their response and movements to external or internal signal sources such as oxygen, gravity, and light. However, the movements of microorganism transport cannot be explained by using mass transfer classical theory. Therefore, it is essential to formulate the microorganisms transport equation based on the laws of biology and fluid mechanics to investigate the motion of microorganisms.

### 1.1.6 Boundary Layer Theory

A boundary layer is a thin region near the body surface. The particle of fluid moves and sticks to the wall due to its viscosity. Prandtl introduced  $x$  and  $y$  as the scaled counterparts of the physical coordinates,  $u$  and  $v$  are dimensionless counterparts of the physical velocity components in the  $x$  and  $y$  directions, respectively, and  $L$  as a reference length. The flow velocity varies from zero at the surface up to the external velocity,  $U_e$  (the maximum value is 1) at the boundary. This phenomenon created a boundary layer thickness,  $\delta$  as shown in Figure 1.4. The boundary layer thickness,  $\delta$  is the distance across a boundary layer from the wall to a point where the flow velocity has substantially reached the free stream velocity,  $U_e$ . This distance is defined normal to the wall, and it is customarily defined as  $u(\delta) = 0.99U_e$  (Schlichting et al., 1955; Çengel and Cimbala, 2006).

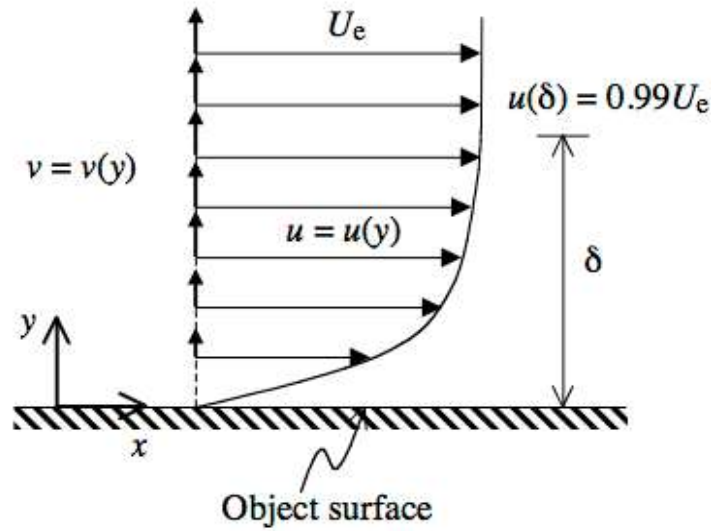


Figure 1.4 Boundary layer profile (Groh, 2012)

For boundary layer approximation theory, Prandtl suggested two constraints to reduce the governing equations. First, the viscous layer must be thin relative to the characteristics streamwise dimension of the object immersed in the flow,  $\delta^* / L \ll 1$  ( $\delta^*$  is the thickness of boundary layer). Second, the largest viscous term must be of the same approximate magnitude as any inertia (particle acceleration) term. Prandtl used the order of magnitude analysis to simplify the governing equations (Schlichting et al., 1955) and found that the second derivatives of the velocity components in the streamwise direction were negligible compared to the corresponding derivatives transverse to the main flow direction. Therefore, the Prandtl boundary layer approximation is used to reduce general governing equations to boundary layer equations (Pletcher et al., 2012). The boundary layer equations that governed the flow characteristics are continuity, momentum, energy, nanoparticle mass concentration, and microorganism equations. The detailed derivations to derive these equations are shown in Chapter 3.



### 1.1.7 Dimensionless Numbers

#### Reynold Number (Re)

$$\text{Re} = \frac{U_r L}{\nu} \quad (1.1)$$

According to Çengel and Cimbala (2006), the Reynolds number measures the ratio of the inertia force to the viscous force. It indicates the thickness of the velocity boundary layer. The viscous forces exceed the inertia forces if  $\text{Re} < 1$ , characterises the flow as laminar and smooth. Meanwhile, if  $\text{Re} > 1$ , the inertia forces exceed the viscous forces and the flow is classified as turbulent. The inertia forces are equivalent to the viscous forces as  $\text{Re} = 1$ . The transition from laminar to turbulent flow occurs if the Reynolds number exceeds a certain critical value called the critical Reynolds number. For example, the critical Reynolds number for flow inside a circular pipe is about 2300, while the critical Reynolds number for a flow in a boundary layer along a flat plate is in the range of  $3.5 \times 10^5$  to  $1 \times 10^6$ .

#### Prandtl Number (Pr)

$$\text{Pr} = \frac{\nu}{\alpha} = \frac{\mu C_p}{k} \quad (1.2)$$

The Prandtl number is the ratio of the kinematic viscosity to the thermal diffusivity (Schlichting et al., 1955). For a small value of  $\alpha$ , the thin layer near the wall in which the temperature distributions varies sharply and will be affected by heat conduction is known as the thermal boundary layer. If  $\text{Pr} < 1$ , the development of the thermal boundary layer is faster than the momentum boundary layer and if  $\text{Pr} > 1$ , the development of the thermal boundary layer is slower than the momentum boundary

layer. If  $Pr = 1$ , the kinematic viscosity is equal to the mass diffusivity. Therefore, Prandtl number plays an important role in controlling the heat conduction and viscosity of the fluid. It provides a measure of the fluid ability to transport the momentum and energy (Uddin, 2013).

### **Lewis Number (Le)**

$$Le = \frac{\alpha}{D_B} \quad (1.3)$$

The Lewis number measures the ratio of thermal diffusivity to mass diffusivity. It is used to characterise fluid flows where there are simultaneous heat and mass transfer by convection (Uddin, 2013). The Lewis number is therefore a measure of the relative thermal and nanoparticle mass boundary layer thickness as can be expressed in terms of the Schmidt number (Sc) and the Prandtl number (Pr) as  $Le = \frac{Sc}{Pr}$ .

### **Bioconvection Lewis Number (Lb)**

$$Lb = \frac{\alpha}{D_n} \quad (1.4)$$

The bioconvection Lewis number measures the ratio of thermal diffusivity to microorganism diffusivity (Kuznetsov, 2011). It is used to characterise fluid flows where there are simultaneous heat and microorganism transfer by convection. It can also be expressed in terms of the bioconvection Schmidt number (Sc) and the Prandtl number (Pr) as  $Lb = \frac{Sb}{Pr}$ .

### **Peclet Number (Pé)**

$$Pe = \frac{\tilde{b}W_c}{D_n} \quad (1.5)$$

The Peclet number measures the ratio of flow advection to the rate of swimming diffusion (Kuznetsov, 2011). The Péclet number, Pé characterises the relative importance of advection and diffusion influences on the microorganism distribution.

### **Bioconvection Rayleigh Number (Rb)**

$$Rb = \frac{\gamma(n_w)_0(\rho_m - \rho_f)}{\beta((T_w)_0 - T_\infty)(1 - C_\infty)\rho_f} \quad (1.6)$$

The bioconvection Rayleigh number measures the concentration of microorganisms due to buoyancy force (Kuznetsov, 2011). It characterises the existence and strength of bioconvection within the suspension, and the magnitudes represent the stabilising or destabilising effect on the system.  $Rb = 0$ , corresponds to a suspension with no microorganism. The increase of Rb thus destabilises the suspension.

### **Skin Friction Coefficient**

The dimensionless shear stress on the surface of a body due to fluid motion is known as local skin friction factor and is defined as (Uddin, 2013):

$$C_f = \frac{2\tau_w}{\rho U^2} \quad (1.7)$$

where  $\tau_w = \mu \left( \frac{\partial \bar{u}}{\partial y} \right)_{\bar{y}=0}$  is the local shearing stress on the surface of the body.

## Nusselt Number

The Nusselt number measures the ratio of convective to conductive heat transfer coefficients across the boundary layer (Uddin, 2013). In industrial applications, the information on the quantity of heat exchange is much more important than velocity and temperature field. The quantity of heat exchange  $h(\bar{x})$  can be calculated with the help of heat transfer coefficient which is defined by Newton's law of cooling. If  $q(\bar{x})$  is the quantity of heat exchanged between the wall and the fluid per unit area, per unit time at a point  $\bar{x}$ , then according to Kuznetsov (2011):

$$q = h(\bar{x})(T_w - T_\infty). \quad (1.8)$$

Since the heat exchanged between the body and the fluid at the boundary is only due to conduction, and according to Fourier's law:

$$q_w = k \left( \frac{\partial T}{\partial n} \right)_{n=0} \quad (1.9)$$

where  $n$  is normal to the surface of the body. The following dimensionless coefficient, known as the Nusselt number, can be defined by combining these two laws:

$$Nu = \frac{hL}{k} = \frac{q_w L}{k \Delta T}. \quad (1.10)$$

A parallel expression can be defined for mass, and microorganism transfers rate called the Sherwood and microorganism number, respectively.

### 1.1.8 Slip Boundary Conditions

Previous studies in many cases use no-slip boundary conditions to model the boundary layer fluid flow. The no-slip boundary is a condition at a solid boundary where fluid in motion comes to a solid boundary and assumes a zero velocity relative to the boundary. However, as nanoscale flow is seldomly considered (e.g. hard disk drives, micro-pumps, micro-valves and micro-nozzles), many researchers realised that the most appropriate way to model the boundary layer flow is by using slip boundary conditions (associated with the inclusion of velocity, temperature, and microorganism slips). The situations occur with slip and no-slip conditions in the boundary layer flow for velocity, temperature, nanoparticle mass, and microorganism are shown in Figure 1.5 and Figure 1.6, respectively. In addition, boundary layer flow should be modelled using slip conditions especially if the non-Newtonian fluid is being considered. This is due to the existence of nonlinear relation between the slip velocity and the traction in non-Newtonian fluid (Uddin et al., 2016a).

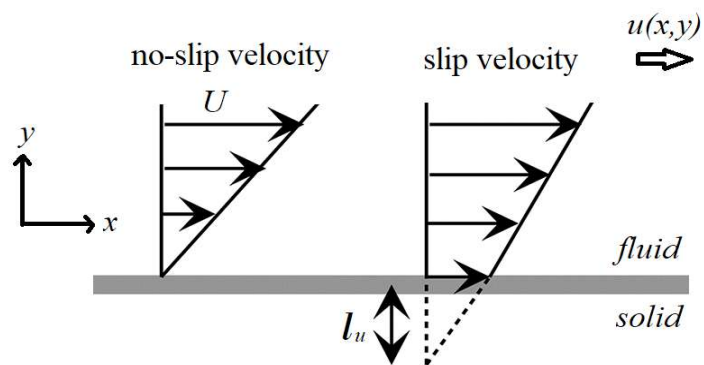


Figure 1.5 The difference between no-slip velocity and slip velocity boundary layers (Maynes and Crockett, 2014)

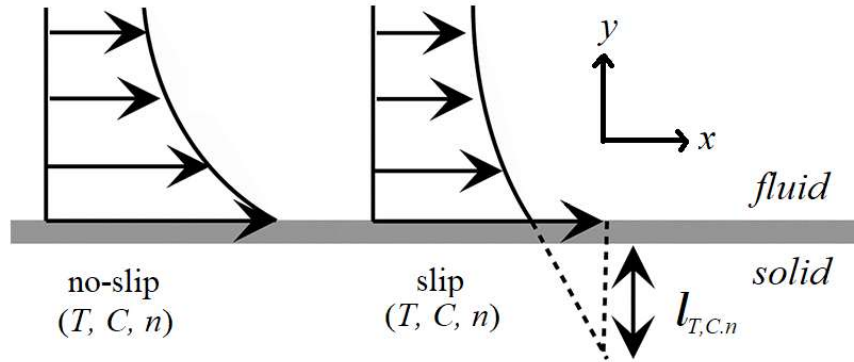


Figure 1.6 The difference between no-slip (temperature, nanoparticle mass and microorganism) and slip (temperature, nanoparticle mass and microorganism) boundary layers (Maynes and Crockett, 2014)

### 1.1.9 Stefan Blowing Boundary Condition

In microfluidics material processing applications, it is sometimes assumed that the surface boundary contains tiny holes. Then it is essential to include Stefan blowing effects in the model (Uddin et al., 2016a). Stefan blowing is the situations where extensive diffusion of mass to the ambient can occur (Rosner, 2012). It should be noted that mass diffusion depends on the flow field that exists due to mass blowing at the wall. The theory of blowing effect can be adopted from Stefan problem, which is different from the permeable surface in mass injection or blowing due to transpiration (Fang, 2014). Stefan blowing is the ideal boundary condition to model the mass transfer in a viscous fluid under high flux conditions (Fang and Jing, 2014). Stefan blowing parameter in the boundary condition provides a correction factor in the conservation equations. Fang (2014) investigated such type of flow past a stretching sheet and found that blowing effect due to the mass transfer could influence the velocity, drag, heat flux, temperature, and concentration profiles.

## 1.2 Problem Statement

A magnetic field effect plays an essential role to enhance heat, nanoparticle mass, and microorganism transfer in microfluidic devices. According to Tham et al. (2013), another modification that can be made to enhance the mixing process is by introducing nanoparticles and microorganisms into the microfluidic system. As microorganism is introduced into a model, the unsteady analysis needs to be considered due to the assumptions that the concentration of microorganisms is high. It is based on the observations from the experimental results which reported that unsteady convection analysis is needed to observe the collection of cloudy plumes microorganism as the concentration increased (Vadász, 2008). Nowadays, as the flow at the nanoscale is considered (e.g. hard disk drives, micro-pumps, micro-valves and micro-nozzles), many researchers realised that the most appropriate way to model the boundary layer flow is by using slip boundary conditions (associated with the inclusion of velocity, temperature, and microorganism slips). In terms of the type of fluids, there are situations that fluid cannot be easily represented or modelled as viscous fluid under Newton's law of motion or by the Navier-Stokes equations. They have special characters such as small body fluids and colloidal fluid element that need to be considered in understanding the motion of the fluid flow (Hussanan et al., 2017). Hence, in microfluidics material processing applications, it is sometimes assumed that the surface boundary contains tiny holes. It is essential to include Stefan blowing effects on the model (Uddin et al., 2016a). Therefore, this thesis aims to fill the research gap by developing a mathematical model of microfluidics flows especially in relation to heat, nanoparticle mass, and microorganism transfers and use the model to understand the associated phenomena and effects. The physical problems that will be investigated in this thesis are:

1. The stretching/shrinking disk, Stefan blowing and multiple slips effects on the skin friction, heat, nanoparticle mass and microorganism transfers over a rotating disk.
2. The squeezing parameter, Stefan blowing and multiple slips effects on the skin friction, heat transfer, mass transfer and microorganism transfer between two parallel disks.
3. The mixed convection parameter, Stefan blowing and multiple slips effects on the skin friction, heat, nanoparticle mass and microorganism transfers past a vertical rotating cone.
4. The stretching/shrinking sheet, Stefan blowing and multiple slips effects on the skin friction, heat, nanoparticle mass and microorganism transfers.

The lack of such mathematical models and the inability to solve such models accurately and efficiently impede the understanding of increasingly important heat, nanoparticle mass, and microorganism transfers phenomena. For this purpose, it is essential for the researchers who work in this area to understand the flow problems.

### **1.3 Research Objectives and Scope**

The objectives of this thesis are:

- 1) To formulate the mathematical models of unsteady boundary layer flow over various geometries and subject to multiple slips and Stefan blowing boundary conditions.



- 2) To transform the partial differential equation into ordinary differential equations using suitable similarity variables.
- 3) To solve the mathematical models numerically using Maple software.
- 4) To investigate the numerical results obtained to study the fluid flow, heat transfer, mass transfer, and microorganism transfers.

The scope in this study was narrowed down into the unsteady of a viscous incompressible laminar boundary layer nanofluid flow with the magnetic field, Stefan blowing and slip effects. The unsteady situations, such as self-induced motions of the body, fluctuations, non-uniformities in the surrounding fluid, need to be taken into account. Lorentz force that is considered to represent the effect of MHD in the mathematical models consists of electric field and magnetic field. In this thesis, it is assumed that there is no polarised or applied voltage enforced on the fluid flow which imposes the zero electric fields. The magnetic Reynolds number of the flow is taken to be small enough so that only magnetic field influences the Lorentz force.

The water-based fluid is chosen to satisfy the physical requirement for the survival of microorganisms (Das et al., 2015). It is assumed that the nanoparticles do not agglomerate and the suspension remains stable. In addition, the presence of nanoparticles is assumed to have no effect on the direction in which microorganisms swim, and on their velocity. Bioconvection-induced flow took place in a dilute suspension of nanoparticles (Khan et al., 2014). This assumption is justified only when the nanoparticles' concentration is less than 1% (Das et al., 2015). The suspension's viscosity is related to the concentration of nanoparticles, the bioconvection is suppressed once the viscosity becomes large enough (Kuznetsov, 2011). The Stefan blowing at the wall is assumed, due to impermeable and the blowing velocity that is

solely determined by the mass transfer at the wall (Fang, 2014). On the contrary, slip boundary condition is considered because slip appears to be more acceptable than that of no-slip for microfluidics applications. Moreover, no slip condition is a particular case of slip condition, with the magnitude of slip equals to zero (Chakraborty, 2009).

Using a similarity transformation, the dimensional form of governing partial differential equations is then transformed into ordinary differential equations. In order to solve the dimensionless form of ordinary differential equations, the finite difference method with Richardson extrapolation is implemented in each of the case studied. Richardson's extrapolation is used to obtain higher order accuracy of the nonlinear two-point boundary value problem.

#### **1.4 Research Methodology**

The research methodology is as shown in Figure 1.7. Transport problems involving unsteady MHD boundary layer nanofluid flow with microorganism, over various geometries subjected to multiple slips and Stefan blowing boundary conditions are first formulated. The dimensional form of governing partial differential equations is then transformed into ordinary differential equations using similarity variables. The transformed governing equations with relevant boundary conditions are solved using numerical methods. The results are then validated by comparing with the previous literature. Lastly, the quantities of physical interest were assessed in detail using the numerical data generated.

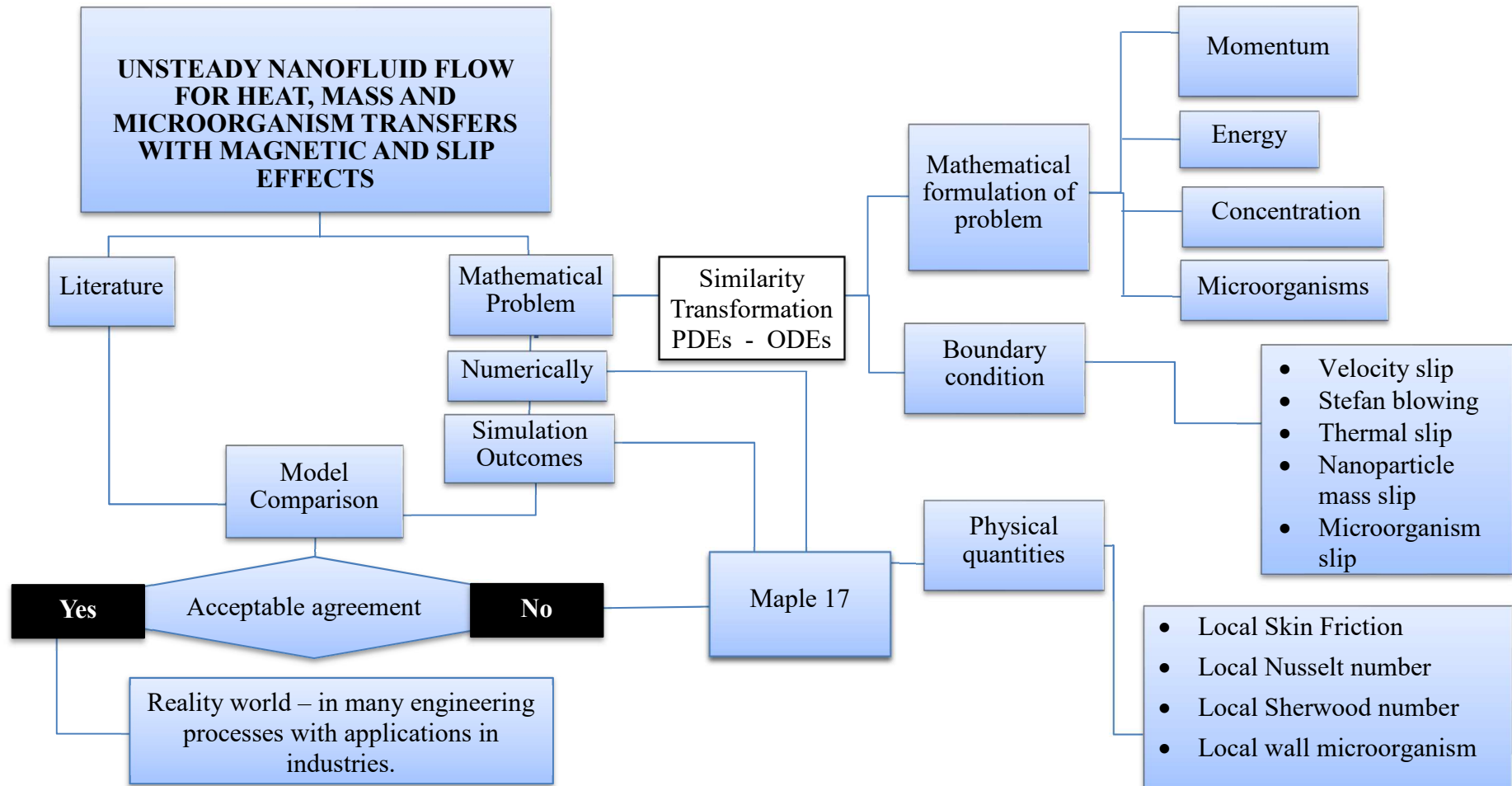


Figure 1.7 Research framework

## 1.5 Significance of Study

The study of flow problems with the magnetic field, nanofluid, and microorganism are important especially in microfluidic devices. The advantages of microfluidic devices are its small size, low cost, and low consumption, as it does not involve the use of various costly equipment or apparatus especially for biological studies. A specific device has been developed to improve the microscale and nanoscale capabilities in mechanobiology of platelets application. The microfabricated device is adaptable to control physical and nanometer-scale interactions for studying platelets under shear flow (Fegghi and Sniadecki, 2011). The applications such as mixing, pumping, sorting of particle and cells, and the enhancement of heat and mass transfer phenomena could be manipulated using nanofluid and magnetic field effects. The combination of such effects contributes to a low cost, efficient, and versatile technology for a number of microfluidic device applications. Therefore, it is important to improve the understanding on the microfluidic flow system to achieve efficiency and high throughput. Moreover, the effective systems depend on the right geometry for the devices. Therefore, the knowledge to understand the flow behaviour, heat transfer, mass transfer and microorganism transfer with various geometries are vital for this purpose.

In the present study, the behaviour of nanofluid flow, temperature, nanoparticle mass, and microorganism with Stefan blowing and multiple slips effects over various geometries can be determined. Moreover, a clear understanding on the flow through the system with the presence of MHD and several controlling parameters can be explicitly provided in terms of mathematical background. In addition, complete knowledge on physical quantities such as heat, nanoparticle mass, and microorganism

transfer rates relevant to the large-scale engineering applications are presented. Mathematically, the use of similarity transformations and numerical methods are essential for detailed analysis and in understanding the significant correlations between the dependent and independent dimensionless groups in flow and transport processes. The relevant results produced from the present study can help engineers in decision making for many transport processes and viscous flow phenomena. Accurate solutions produced from the numerical studies could increase the understanding on the existing and future industrial processes, highlighting the most significant impact of the present study.

## **1.6 Outline of Thesis**

This thesis comprises of eight chapters including the introductory chapter. The introductory chapter provides a detailed description of the research background, problem statement, research objectives and scope, research methodology, and the significance of the study. The literature review in Chapter 2 surveys previous studies related to the topics in this research. Chapter 3 discusses the basic concepts of transport phenomena for each problem and the relevant effects incorporated into the models.

In Chapter 4, the unsteady MHD forced convection over rotating stretchable/shrinkable disk immersed in a nanofluid containing microorganisms is discussed. In this chapter, four different cases occurred on the rotating disk system were considered, namely the shrinking disk with suction case, the shrinking disk with blowing case, the stretching disk with suction case, and the stretching disk with blowing case. The graphs are plotted and discussed for various controlling parameters

such as the unsteadiness parameter, magnetic field parameter, multiple slips parameter, Lewis number, bioconvection Lewis number, and Péclet number.

In Chapter 5, the unsteady MHD forced convection of squeezing nanofluid flow with microorganism between two parallel disks subjected to Stefan blowing and multiple slips effects are taken into account. In this chapter, four different cases occurred on the upper and lower disks system are considered. The cases are: (1) the upper disk moves closer to the stationary lower disk with suction effect on the lower disk, (2) the upper disk moves closer to the stationary lower disk with blowing effect on the lower disk, (3) the upper disk moves apart from the stationary lower disk with suction effect on the lower disk, and (4) the upper disk moves apart from stationary lower disk with blowing effect on the lower disk.

In Chapter 6, the unsteady MHD mixed convection nanofluid flow containing microorganism over a vertical rotating cone is considered. The effect of the controlling parameters on the dimensionless tangential and azimuthal velocities, temperature, nanoparticle mass (concentration), the density of motile microorganisms, as well as on the local skin friction, local Nusselt, Sherwood, and motile microorganism numbers for each case are discussed.

In Chapter 7, the unsteady MHD mixed convection of micropolar nanofluid flow with microorganism over a stretching/shrinking sheet is considered. In this chapter, four different cases of micropolar fluid flow system over a sheet are considered, namely the shrinking sheet with suction case, shrinking sheet with blowing case, stretching sheet with suction case, and stretching sheet with blowing case. The numerical results have been plotted for various emerging parameters such as the mixed convection parameter, unsteadiness parameter, buoyancy ratio parameter,

bioconvection Rayleigh number, and magnetic field parameters. Lastly, the thesis is summarised in Chapter 8 together with the recommendation for future work.

## **CHAPTER 2**

### **LITERATURE REVIEW**

#### **2.1 Introduction**

This chapter discusses previous studies related to the topics in this research. This chapter consists of five sections. Sections 2.2, 2.3, 2.4 and 2.5 discuss the literature related to MHD and slip effects over rotating disk, over squeezing flow between two-parallel disks, over a vertical rotating cone, and in micropolar fluid flow over stretching/shrinking sheet, respectively. The last section of this chapter (Section 2.6) examines previous studies relevant to Stefan blowing effect over viscous fluid flow.

#### **2.2 Flow over Rotating Disk**

Many researchers have studied the fluid flow due to rotating disk as it has many applications in engineering processes and industries (e.g. water treatment plant, sports disk, fans, centrifugal pumps, rotors, spinning disk reactors, and other rotating systems). Steady and incompressible viscous fluid flow in rotating disk system with appropriate transformations was firstly investigated by Kármán (1921), and has been widely discussed in many classical books (Schlichting et al., 1955; White, 2006; Pantan, 1984; Rosenhead, 1963). Cochran (1934) reconsidered Kármán (1921) problem and presented more reliable numerical results. Since then, many researchers have studied the unsteady rotating disk. According to Attia (2006), the unsteadiness should be taken into account due to the angular velocity of the rotating disk which varies with time. Benton (1966) developed a mathematical model on the unsteady case of rotating disk. Representative studies dealing with rotating disks system with